The influence of the interlayer exchange coupling on the magnetism of an Fe(001) monolayer

T. Ślęzak [a,*], M. Ślęzak [a], K. Matlak [a], R. Rohlsberger [b], C. L'Abbe [c], R. Rüffer [d], N. Spiridis [e], M. Zając [a], J. Korecki [a,e]

[a] *Faculty of Physics and Applied Computer Science, AGH University of Science and Technology, Al. Mickiewicza 30, 30-059 Kraków, Poland*
[b] *Hamburger Synchrotronstrahlungslabor, Deutsches Elektronen Synchrotron, 22607 Hamburg, Germany*
[c] *Instituut voor Kern- en Stralingsfysica, K.U.Leuven, Celestijnenlaan 200D, B-3001 Leuven, Belgium*
[d] *European Synchrotron Radiation Facility, Boîte Postale 220, 38043 Grenoble Cedex, France*
[e] *Institute of Catalysis and Surface Chemistry, Polish Academy of Sciences, Niezapominajek 8, 30-239 Kraków, Poland*

Available online 24 April 2007

Abstract

We investigated changes in the magnetic properties of a single Fe monolayer on Au(001) induced by the interlayer exchange coupling (IEC) to FeAu monoatomic superlattices. The grazing incidence nuclear resonant scattering of X-rays (GI-NRS) combined with the ^{57}Fe probe layer concept allowed us to selectively monitor the local structure and magnetism of the Fe(001) monolayer in a coupled state. The dependence of the monolayer hyperfine parameters on temperature and spacer thickness was determined from the fitted GI-NRS time spectra, collected for the selected thickness of the stepped Au spacer. The influence of the coupling on the hyperfine magnetic field B_{HF} was negligible at temperatures much lower than T_C of the uncoupled Fe monolayer ($T_C = 210$ K as checked by MOKE). The analysis of the time-spectra accumulated at 200 K showed a non-monotonous dependence of the average B_{HF} as a function of the spacer thickness, related to IEC oscillations. The maximum influence of IEC on B_{HF} (13 T) was found for the 4 ML Au spacer.
© 2007 Elsevier B.V. All rights reserved.

Keywords: Epitaxy; Interlayer exchange coupling; Curie temperature; Synchrotron radiation; Mössbauer spectroscopy

1. Introduction

The interlayer exchange coupling (IEC) is one of the most exciting phenomena observed in nano-layered magnetic materials. Whereas its nature and consequences, such as artificially structured ferro- or anti-ferromagnetism, giant magnetoresistance, etc., are rather well known and understood, the influence of the coupling on the collective magnetic properties of the whole multilayer system and its individual constituents is still not clear. In particular, for a trilayer system composed of two different ferromagnetic layers (FM1 and FM2) separated by a metallic, non-magnetic spacer (NM), there are two important issues concerning the ferromagnetic sub-layers which are addressed experimentally [1], and theoretically [2], namely: (i) the existence of two different Curie temperatures in the exchange coupled FM1/NM/FM2 system and (ii) the IEC induced shift of the Curie temperature of the ferromagnetic sub-layers with respect to their uncoupled state value. The above phenomena can be favorably observed when the Curie temperature of one of the FM layers (in the uncoupled state) is much lower as compared to the other. This can be achieved by an appropriate choice of materials and their thicknesses as it was done, for example, for the Co/Cu/Ni trilayers [1]. For ultrathin films, the Curie temperature depends strongly on thickness, and thus, upon approaching the single monolayer thickness limit, one often finds the Curie transition well below room temperature [3].

---

* Corresponding author. Tel.: +48 12 6173583; fax: +48 12 6341247.
  E-mail address: slezak@uci.agh.edu.pl (T. Ślęzak).

The Fe monolayer grown on Au(001) was regarded as one of the best understood model monolayers with regard to its magnetic and structural properties [4]. This opinion was related to the almost ideal two-dimensional Fe growth induced by gold self-surfactant action. Later, STM and LEED studies proved that, at the initial stages of the iron growth, the monolayer of Au automatically diffuses onto the growing Fe film preventing it from breaking up into islands [5,6]. On the other hand, the same mechanism is responsible for the pronounced intermixing of Au and Fe which, in turn, results in a complicated Fe monolayer structure, as shown recently by conversion electron Mössbauer spectroscopy (CEMS) [7]. The magnetic properties of the Fe monolayer, such as ferromagnetism and strong perpendicular magnetic anisotropy (PMA), are also characteristic of the monoatomic FeAu superlattices $(Fe_1Au_1)_n$, in which the Fe monolayer is a basic unit [8]. In the case of FeAu monoatomic multilayers $(Fe_1Au_1)_n$, the layer-by-layer growth by molecular beam epitaxy (MBE) stabilizes the $L1_0$-type ordered phase that does not exist in the Fe–Au phase diagram. The magnetic domain structure of the $(Fe_1Au_1)_n$ superlattices depends strongly on the repetition number n varying from a complex stripe domain pattern observed for high n values to a single domain state for lower n [9].

In our experiment, we investigated changes in the magnetic properties of the single Fe monolayer on Au(001) induced by the IEC to $(Fe_1Au_1)_3$ monoatomic superlattices.

2. Sample preparation and characterization

The samples were grown by MBE under UHV conditions (the pressure during preparation was below 10^{-9} mbar), at room temperature, on a 30 nm Au(001) buffer layer with the so-called hex-type surface reconstruction, deposited on atomically smooth, and polished MgO(001) substrates in a multistage process [5]. The thickness of the layers was controlled by a quartz microbalance with an accuracy of about 5%. The sample growth was monitored in situ by low energy electron diffraction (LEED). The magnetic properties were studied ex situ using the magneto-optic Kerr effect (MOKE) and grazing incidence nuclear resonant scattering of X-rays (GI-NRS).

The studied system is shown in Fig. 1. First, on the Au(001) buffer, a ^{57}Fe monolayer was deposited. Then, using a moveable shutter, a stepped spacer layer Au_N with a thickness ranging from $N = 3$ to 7 monolayers (MLs) in one monolayer steps (1ML Au = 2.04 Å) was evaporated. The step width was 1 mm. On the spacer, a monoatomic $(^{56}Fe_1Au_1)_3$ superlattice was prepared by alternating evaporation of ^{56}Fe(001) and Au(001) atomic layers, while we kept a part of the previously prepared system shuttered to allow access to the uncoupled Fe monolayer. Finally, the whole sample was capped with a 2 nm protective Au film. Sharp diffraction spots and low background LEED patterns in all stages of the growth indicated the high degree of structural order. The distinct Au(001)-hex reconstruction of the buffer layer, disappearing during the Fe monolayer growth (at about 0.6 monolayer (ML)), was recovered after deposition of 2–3 ML of the Au spacer. Similarly, reconstruction of the Au spacer layer surface vanished at the very beginning of the $(^{56}Fe_1Au_1)_3$ growth (during deposition of the first Fe monolayer) and reappeared again after the deposition of 2–3 AL of Au capping. The LEED observations indicated that the $(^{56}Fe_1Au_1)_3$ stack was structurally and morphologically homogeneous, independent of the spacer thickness.

Since the small spot size of the laser beam (<0.2 mm) was used in the MOKE experiment, the signal could be taken separately from the different sample steps. The results of the temperature dependent polar MOKE measurements of the uncoupled Fe monolayer are shown in Fig. 2. The magnetization $M(T)$ at a given temperature was estimated by the Kerr rotation at the remanent state derived from the magnetic hysteresis curve. The measured loops were always rectangular and centered, as seen from the inset in Fig. 2, which confirms that the easy magnetization axis is perpendicular to the film plane. The $M(T)$ dependence was fitted to the $M(T) = M(0)(1 - T/T_C)^\beta$ formula. The best fit was obtained for $\beta = 0.180$ and $T_C = 210$ K.

The obtained value of the critical exponent β is considerably higher than expected theoretically from the 2D Ising model ($\beta = 0.125$); it was, however, closer to the value $\beta = 0.22$ reported by Dürr et al. [3], who proposed to explain the deviation from Ising-like behavior (strictly valid only for short range, nearest-neighbors interactions) by
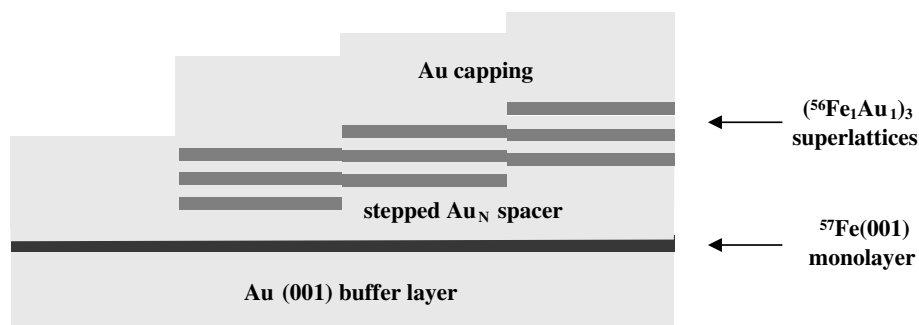

Fig. 1. Schematics of the $^{57}Fe_1/Au_N/$ $(^{56}Fe_1Au_1)_3$ system grown on an Au(001) buffer and covered with an Au capping layer.
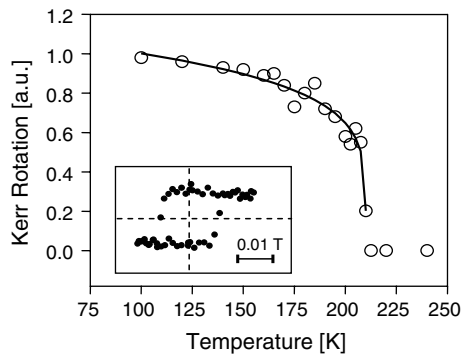
Fig. 2. Magnetization vs. temperature dependence measured by PMOKE for the uncoupled Fe(001) monolayer grown on an Au(001) buffer and capped with 2 nm of Au. The solid line represents the theoretical fit. The inset shows the hysteresis loop measured at 180 K.

contributions from the long range interaction (for example, the *RKKY* type). For the sample steps forming $^{57}Fe_1/Au_N/$ $(^{56}Fe_1Au_1)_3$ trilayers, the Kerr loops were always rectangular (independently of T), indicating a ferromagnetic IEC in the investigated spacer thickness range, in agreement with our previous experiment [9]. It has to be pointed out that, for $^{57}Fe_1/Au_N/(^{56}Fe_1Au_1)_3$ trilayers, the Kerr signal was dominated by the contribution from $(^{56}Fe_1Au_1)_3$ blocks (having T_C well above RT) and, thus, the Fe monolayer magnetic properties (magnetization, T_C) could not be directly probed.

3. GI-NRS experiment

For selective studies of the Fe(001) monolayer properties, the isotopic sensitivity of the grazing incidence nuclear resonant scattering of X-rays (GI-NRS) was exploited [10]. The method is similar to classical Mössbauer spectroscopy (MS) in the sense that recoilless excitation of the nuclear energy levels split due to the hyperfine interactions is involved. In combination with the ^{57}Fe probe layer concept, the method gives local structural and magnetic information from a sample region pre-selected during the sample preparation. Since GI-NRS is not sensitive to the $(^{56}Fe_1Au_1)_3$ stack, all of the information derived from the measured time spectra can be related to the $^{57}Fe(001)$ monolayer. In this method, the hyperfine parameters can be obtained from a characteristic beat pattern seen in the time evolution of the nuclear resonant scattering (time spectrum) [11]. Due to high brilliance of the third generation synchrotron sources, it provides unique possibilities to probe magnetic properties with sub-monolayer sensitivity. Moreover, fine focusing of the synchrotron X-ray beam enables studies of wedge-shaped systems, which is not possible in the case of MS experiments, which require large area samples. The GI-NRS measurements were performed at the ID22N beam line in ESRF Grenoble. The samples were mounted in a He cryostat and oriented with the Au spacer step edges parallel to the direction of the X-ray propagation. The X-ray beam was focused horizontally to 50 μm to ensure good

separation between sample areas with different spacer thicknesses. The grazing incidence angle (~3.8 mrad) was optimized for the maximum count rate of the delayed quanta intensity. In the temperature dependent GI-NRS investigations, the time spectra were collected for the different sample positions relative to the X-ray beam, corresponding to the selected thickness of the Au spacer and, thus, the influence of the coupling on the Fe monolayer magnetic state was probed. The GI-NRS data were fitted using the program CONUSS [12]. The time spectrum of the uncoupled Fe monolayer collected at 80 K is shown in Fig. 3a. A satisfactory fit was obtained assuming three magnetic components characterized by the magnetic hyperfine field distributions (HFDs). The direction of all hyperfine magnetic fields B_{HF} was along the film normal confirming perpendicular magnetic anisotropy of the Fe monolayer. Interpretation of the beat pattern in terms of hyperfine parameters, as well as the relative contributions of the fitted components, agrees with the CEMS results of the Fe(001) monolayer grown on Au(001) [7]. In particular, the true monolayer sub-spectrum was identified by its large quadruple splitting QS = 0.4 mm/s. Its contribution was estimated as almost 40%. The remaining two sub-spectra correspond to the double layer patches and Fe atoms in the substitutional Au–Fe alloy. The complex structure of the nominal Fe(001) monolayer can be also responsible for the higher value of the critical exponent β, as it was found from the PMOKE measurements. At low temperatures, the time spectra measured for the coupled Fe monolayer were very similar and, within the statistical error,
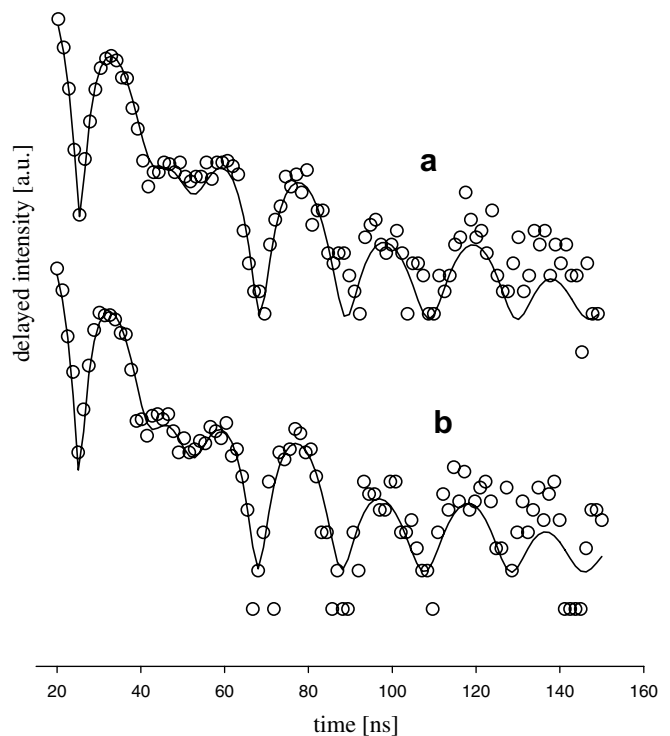

Fig. 3. Time spectra collected at 80 K for (a) the uncoupled ^{57}Fe monolayer and (b) for the $^{57}Fe_1/Au_4/(^{56}Fe_1Au_1)_3$ system. The solid lines represent theoretical fits.

could be fitted with the same set of parameters, indicating negligible influence of IEC (see, for comparison, GI-NRS data of $^{57}Fe_1/Au_4/(^{56}Fe_1Au_1)_3$ shown in Fig. 3b). This situation changes as the Fe monolayer Curie temperature is approached.

In Fig. 4, the time spectra measured for the system at 200 K are shown. Similar to the 80 K data, the fits were obtained assuming three spectral components. All spectra were fitted simultaneously with the magnetic hyperfine field values and their HFDs as the only independent parameters.
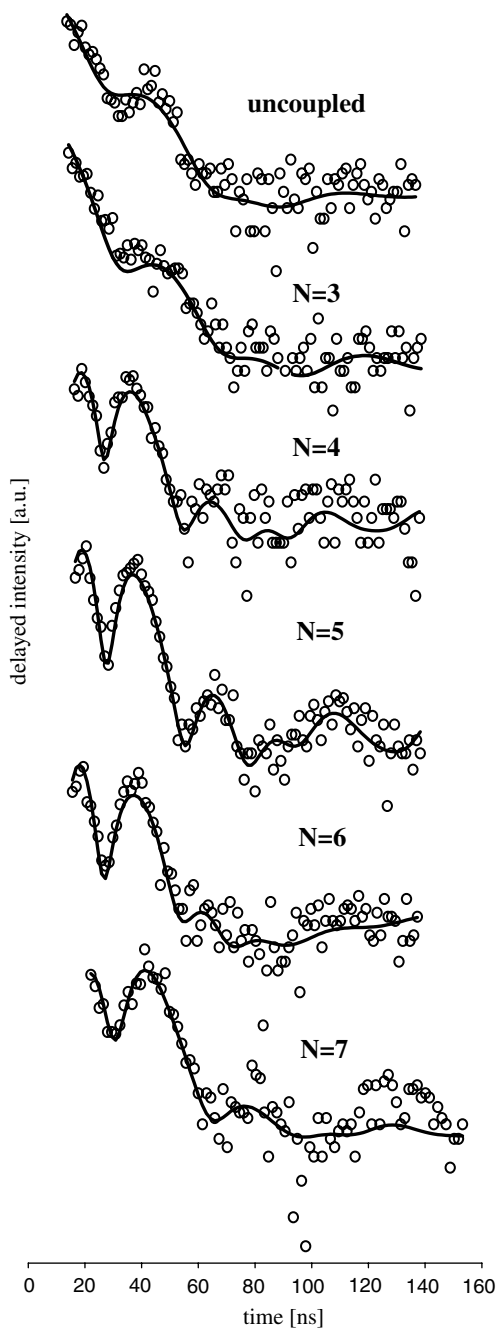
The other parameters, such as chemical shift, quadruple splitting, and relative subspectra contributions (describing local structure), were treated consistently. In such a model, B_{HF} and its distribution are a measure of the local magnetization averaged on the scale given by the characteristic time window of the method (10^{-8} s) [10]. Despite the large spread of the data for times greater than 100 ns, good statistical quality of the spectra at earlier times and the fitting procedure using a weighted χ^2 test yields B_{HF} values within 0.1 T accuracy. In Fig. 5, the average hyperfine magnetic field $\langle B_{HF} \rangle$ calculated from the fit parameters is shown as a function of the spacer thickness. The dashed line marks the uncoupled Fe monolayer average hyperfine field ($\langle B_{HF} \rangle = 5.6$ T). It is clear that a change of the $\langle B_{HF} \rangle$ vs. the spacer thickness is non-monotonous, reflecting changes of the IEC strength, which is ferromagnetic in the studied spacer thickness range. Surprisingly, the close proximity of the magnetic layer ($N = 3$) does not lead to the maximal hyperfine magnetic field enhancement. The maximum $\langle B_{HF} \rangle = 18.6$ was found for the 4 ML of Au spacer and, for the thicker $\langle B_{HF} \rangle$, clearly decreases.

The observed effects close to the transition temperature were discussed before as a shift of the Curie temperature [1]. Unfortunately, limited time of the synchrotron experiment restricted the number of temperature points at which the time spectra could be measured. Therefore, a dependence of the monolayer Curie temperature on the spacer thickness could not be directly derived.

The above analysis is based on a static reduction of the magnetic moments with increasing temperature. At the temperatures close to the magnetic phase transition, a spin fluctuation picture would be more appropriate, requiring dynamical fitting of the time spectra when the spin fluctuation frequency is comparable with the Larmor frequency of the nuclear magnetic moment. This could give direct confirmation that the IEC influence on the monolayer mag-
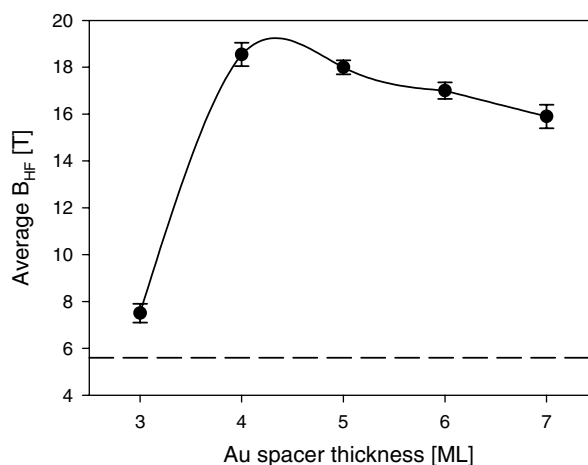

Fig. 4. Time spectra collected at 200 K for the uncoupled Fe monolayer and $^{57}Fe_1/Au_N/(^{56}Fe_1Au_1)_3$ system. The spacer thickness measured in the number N of Au(0 0 1) monolayers is shown.

Fig. 5. Average hyperfine magnetic field $\langle B_{HF} \rangle$ derived from the time spectra measured for the $^{57}Fe_1/Au_N/(^{56}Fe_1Au_1)_3$ system at 200 K as a function of the Au spacer thickness. The dashed line indicates the uncoupled monolayer value. The solid line is a guide for the eyes only.

netism consists of suppressing spin fluctuations existing in the vicinity of the ferromagnetic–paramagnetic phase transition [13]. The role of the coupling at low temperatures is negligible, which further supports the spin fluctuation picture.

In conclusion, we studied, via the hyperfine spectroscopy, the influence of the IEC on the magnetic properties of an Fe(001) monolayer. Our experiment indicated that the magnetic phase transition of nano-magnets can be tuned by IEC.

Acknowledgements

References

[1] A. Ney, F. Wilhelm, M. Farle, P. Poulopoulos, P. Srivastava, K. Baberschke, Phys. Rev. B. 59 (1999) 3938.
[2] J.H. Wu, T. Herrmann, M. Potthoff, W. Nolting, J. Phys. Condens. Mat. 12 (2000) 2847.
[3] W. Dürr, M. Taborelli, O. Pauli, R. Germar, W. Gudat, D. Pescia, M. Landolt, Phys. Rev. Lett. 62 (1989) 206.
[4] F.J. Himpsel, J.E. Ortega, G.J. Mankey, R.F. Willis, Avd. Phys. 47 (1998) 511.
[5] N. Spiridis, J. Korecki, Appl. Surf. Sci. 141 (1999) 313.
[6] V. Blum, O. Rath, S. Muller, L. Hammer, K. Heinz, J.M. Garcia, J.E. Ortega, J.E. Prieto, O.S. Hernan, J.M. Gallego, A.L. Vazguez de Parga, R. Miranda, Phys. Rev. B. 59 (1999) 15966.
[7] W. Karaś, B. Handke, K. Krop, M. Kubik, T. Ślęzak, N. Spiridis, D. Wilgocka-Ślęzak, J. Korecki, J. Phys. Stat. Sol. 189 (2002) 287.
[8] K. Takanashi, S. Mitani, M. Sano, H. Fujimori, Appl. Phys. Lett. 67 (7) (1995) 1016.
[9] T. Ślęzak, W. Karaś, K. Krop, M. Kubik, D. Wilgocka–Ślęzak, N. Spiridis, J. Korecki, JMMM 240 (2002) 362.
[10] R. Röhlsberger, Nuclear Condensed Matter Physics with Synchrotron Radiation, STMP, vol. 208, Springer-Verlag, Berlin, Heidelberg, 2004.
[11] V. Setz, R. Röhlsberger, J. Bansmann, O. Leupold, K.-H. Meiwes-Broer, New J. Phys. 5 (2003) 47.1.
[12] W. Sturhan, Hyp. Interact. 87 (2000) 149.
[13] P.J. Jensen, K.H. Bennemann, P. Poulopoulos, M. Farle, F. Wilhelm, K. Baberschke, Phys. Rev. B. 60 (1999) 994.